Water Air Soil Pollut (2022) 233:486
https://doi.org/10.1007/s11270-022-05953-7

Characteristics and Sources of PAHs, Hopanes, and Elements in PM_{10} Aerosol in Tulsipur and Charikot (Nepal)

Miloš Zapletal · Pavel Cudlín · Chiranjeewee Khadka · Kamil Křůmal · Pavel Mikuška · Hana Cigánková · Martin Polášek

Received: 9 June 2022 / Accepted: 8 November 2022 / Published online: 19 November 2022

Abstract Concentration of PAHs, hopanes, and elements in PM_{10} aerosol samples was measured in two Nepalese urban centers, Tulsipur (725 m above sea level; 150,000 inhabitants) and Charikot (1,550 m above sea level; 23,000 inhabitants) in the monsoon period (August 2018) and pre-monsoon period (April–May 2019). The 24-h PM_{10} limit value of 50 μg m^{-3} for human health was significantly exceeded at all locations, and the Nepal concentration limit of 150 μg m^{-3} was exceeded at Tulsipur-bus station, Tulsipur-village, and Charikot-hospital in the pre-monsoon season. The average daily PM_{10} and PAHs concentrations showed seasonal variations, with lower concentrations in the monsoon season and the higher values in pre-monsoon season. The average daily PM_{10} and PAHs concentrations in the both sites were 133 μg m^{-3} and 23.8 ng m^{-3} in the pre-monsoon period and 49.6 μg m^{-3} and 2.30 ng m^{-3} in the monsoon period, respectively. The average daily hopane concentration during the pre-monsoon period was 1.40 ng m^{-3} in Tulsipur and 0.70 ng m^{-3} in Charikot. The IndP / (IndP + BghiP) ratio was higher than 0.5 during monsoon period, indicating combustion of biomass and charcoal burning. IndP / (IndP + BghiP) between 0.2 and 0.5 during pre-monsoon season indicates petroleum combustion. Fla / (Fla + Pyr) ratio between 0.3 and 0.5 during pre-monsoon and monsoon periods indicates high proportion of petroleum product combustion. The biomass burning associated with dense traffic in the center of the two cities was the main source of PAHs. The average daily element concentration was 6.80 ng m^{-3} in both locations during the monsoon period.

Keywords PM_{10} · Polycyclic aromatic hydrocarbons · Hopanes · Elements · Meteorological parameters · Nepal environment

M. Zapletal (✉) · P. Cudlín · C. Khadka
Global Change Research Institute CAS, Lipová 9, 370 05 České Budějovice, Czech Republic
e-mail: milos.zapletal@physics.slu.cz

M. Zapletal
Institute of Physics in Opava, Silesian University in Opava, Bezručovo náměstí 1150/13, 746 01 Opava, Czech Republic

K. Křůmal · P. Mikuška · H. Cigánková
Department of Environmental Analytical Chemistry, Institute of Analytical Chemistry of the Czech Academy of Sciences, Veveří 97, 602 00 Brno, Czech Republic

M. Polášek
Silesian Museum in Opava, Nádražní Okruh 31, 74601 Opava, Czech Republic

1 Introduction

Currently, air pollution is one of major environmental problems in developing countries (Saud & Paudel, 2018).

Atmospheric aerosols (Particulate Matter, PM) is an important airborne component with many

environmental impacts such as deterioration of air quality, global climate change, visibility reduction, and smog production (Mikuška et al., 2020; Seinfeld & Pandis, 1998). Various studies have shown a link between increased PM concentration and adverse health effects including allergy, asthma, cardiovascular and respiratory diseases, cancer, and increased mortality (Brunekreef & Holgate, 2002; Kim et al., 2015). The health effects of atmospheric aerosols depend mainly on the particle size, the chemical composition of particles, and solubility of PM components in lung fluid. The size of the particle determines how long the particle remains in the atmosphere and where it subsequently settles in the human airways. PM_{10} particles (i.e., particles with aerodynamic diameter of 10 μm or less) deposit in upper part of respiratory tract while smaller particles such as $PM_{2.5}$ and PM_1 particles, due to their small sizes, are able to penetrate deep into the lungs (Biswas et al., 2020; International Commission on Radiological Protection, 1994).

PM_{10} aerosol originates from different emission sources such as combustion of coal, biomass, gasoline, oil, or diesel fuel. PM_{10} also includes dust from agriculture, wildfires, industrial sources, construction sites, resuspended dust from road and soil, and pollen.

The chemical composition of PM_{10} is very complex consisting, in general, from carbonaceous species, soot, inorganic ions, and elements in variable amounts, depending on their location and emission sources (Seinfeld & Pandis, 1998). Despite the huge number of chemical compounds contained in PM, only a limited number of them is considered hazardous to human health. These potentially harmfull compounds include mostly polycyclic aromatic hydrocarbons (PAHs) and some elements (Cd, Pb, Ni, As, Tl, Hg, etc.) because of their carcinogenic and mutagenic properties (Schroeder et al., 1984; Masiol et al., 2012; Křůmal & Mikuška, 2020; Cigánková et al., 2021a). PAHs are formed largely during the incomplete combustion of organic material at high temperatures (Křůmal et al., 2013), while elements are emitted from variety of emission sources including mainly coal and biomass combustion, traffic, and industry (Mikuška et al., 2020).

PAHs and elements bound to PM may exert an adverse toxic effect only after particle deposition on the lung surface, when the soluble particulate components may be dissolved into the pulmonary surfactant. It is assumed that the soluble fraction of PM components is more relevant to the assessment of human health risks than their total concentration (Cigánková et al., 2021b).

Nepal is one of the fastest growing countries in South Asia (Waldorf, 2018). In the State of Global Air Report 2020, Nepal is listed among the top 10 countries with the highest outdoor $PM_{2.5}$ levels in 2019 (Global Air, 2020). Therefore, air pollution is currently one of Nepal's biggest problems. This is due to the rapid deterioration of the urban environment, which is mainly due to unplanned urbanization, transport development (Majumder et al., 2012), and industrialization. Concentrations of aerosol particles regularly reach levels that have been shown to be hazardous to human health (Gurung et al., 2013). For example, Kathmandu is one of the most polluted cities in Asia due to high concentrations of $PM_{2.5}$ and PM_{10} (Majumder et al., 2012), which regularly exceed United States Environmental Protection Agency (US-EPA) (Giri et al., 2008) and World Health Organization (WHO) (CAI-Asia, 2006; World Health Organization, 2014) limits. Growing population, increasing industry and automobile traffic, heavy deforestation, and forest fires accelerate the deterioration of air quality.

Air pollution by aerosols, NO_2, O_3, etc. can be studied using satellite data produced by the spectrometers MODIS (Moderate Resolution Imaging Spectroradiometer), TROPOMI (Filonchyk & Yan, 2018), etc. (Filonchyk et al., 2018; Biswas et al., 2020; Torres et al., 2020). The satellite instruments provide information about long-term trends of the evaluation and variability of spatial distributions of the total concentrations of aerosols and other pollutants on local or global scales. Alternatively, the aerosols are monitored using ground based instruments that allow the measurement of aerosol concentrations over shorter time intervals and, moreover, the measurement of aerosols in selected size intervals such as size fractions PM_1, $PM_{2.5}$, or PM_{10}.

The research on air pollution from PM_{10} (Giri et al., 2008) and PAH (Chen et al., 2015, 2017) in Nepal is focused mainly on the capital Kathmandu, including the Kathmandu Valley and the area of Himalayan Mountains regions. Emissions and pollutant concentrations (including PM) in Kathmandu area were estimated by atmospheric transport, deposition, and chemistry models (Adhikary et al., 2007).

Another measurement study examined PAH concentrations in PM_{10} in an urban area in the Kathmandu Valley (Kishida et al., 2009). Biomass and fossil fuel combustion especially by vehicles were identified as the main source of polycyclic aromatic hydrocarbons (Yu et al., 2008). Other study showed higher PM concentrations and lead levels in PM samples near roads (Aryal et al., 2008). The highest PM_{10} concentrations were found near industrial centers (Aryal et al., 2008). Concentrations of PM_{10} were typically higher in pre-monsoon (Aryal et al., 2008; Giri et al., 2008).

However, basic available information on atmospheric PM_{10} and its components such as PAHs and elements in the Himalayan Mountains (sources, types, emissions, concentrations, and fate) is still limited (Chen et al., 2015). Several studies described ambient measurements of PM_{10}, or air quality model results for high-altitude areas (e.g. Nepal Climate Observatory Pyramid in the Khumbu Valley (5,079 m a.s.l.)) (Decesari et al., 2010; Giri et al., 2004, 2008; Majumder et al., 2012). The major PM_{10} components have been identified as organics and mineral dust, with combustion being an important source (Decesari et al., 2010). The measurements show temporal patterns. Most pollutants (e.g., $PM_{2.5}$, NO_2) were higher during the pre-monsoon than during the monsoon (Sellegri et al., 2010). Studies showed a regional influence on air quality at high elevations (Bonasoni et al., 2010).

A major limitation in research on the effect of particular matter (PM), PAHs, and elements on human health in Nepal is the lack of exposure data (Gurung et al., 2013). PAHs are hazardous to humans when inhaled (Gong et al., 2011). Therefore, PAHs have received considerable attention owing to their persistence and toxicity, particularly their carcinogenic and/or mutagenic properties (Bhargava et al., 2004; Křůmal & Mikuška, 2020). Ambient monitoring networks maintained by government organizations are required for these purposes. Such data are still not available for the whole of Nepal. Only for PM in the Kathmandu Valley did the Nepalese government routinely measure PM_{10} until 2007 (Gurung et al., 2013). However, information on current levels of particulate matter, including various size fractions, and other pollutants for all Nepal is needed (Gurung et al., 2013) to assess health risks. Such work could include ambient monitoring of PM concentration with alternative, low-cost measurement methods using optical sensors (Kumar et al., 2015; McKercher et al., 2017).

Information on air pollution focusing on particulate PAHs and heavy elements in Nepal is still limited. To extend the knowledge, this study shows the results of monitoring particulate matter (PM_{10}) and bound PAHs, hopanes, and elements in two different Nepalese Urban centers, Tulsipur in the southern part of Nepal in the Teraj area and Charikot in the northern Himalayas, which are highly affected by air pollution. Simultaneously with the measurement of dust particles, continuous data on temperature, relative humidity, global radiation, wind speed, and wind direction were collected directly at the measurement site. Based on these measurements, an overall data analysis was conducted in these areas during the monsoon and pre-monsoon seasons. In addition, we compared PM_{10} concentration measured in parallel by the real-time particle monitor Has-Dust Electronic Pilot Activity and Alertness Monitor (EPAM) 5000 and low-cost sensors in the pre-monsoon season for the possible future use of the sensors in Nepal.

2 Materials and Methods

2.1 Site Description

Tulsipur is the second most populous city in the Nepalese district of Dang with more than 150,000 inhabitants and occupies a municipal area of 385 km^2. The area of Tulsipur is located at an average altitude of 725 m above sea level. Charikot (officially Bhimeshwar) is a smaller town of less than 23,000 inhabitants located in the northeastern part of Nepal's Dolakha district. The town is composed of several neighboring villages and occupies a total area of 70 km^2 at an altitude of about 1,550 m above sea level (Fig. 1).

Nepal is characterized by a subtropical climate with extensive summer monsoon rains between June and early September. The average temperature varies between 12 and 14 °C, with a minimum of about 0 °C during the pre-season and a maximum of about 35 °C during the summer season and varies considerably depending on the altitude. Wind speed averages between 0.4 and 7.5 m s^{-1} and average humidity ranges between 50 and 80% depending on the season (Sill & Kirkby, 2013).

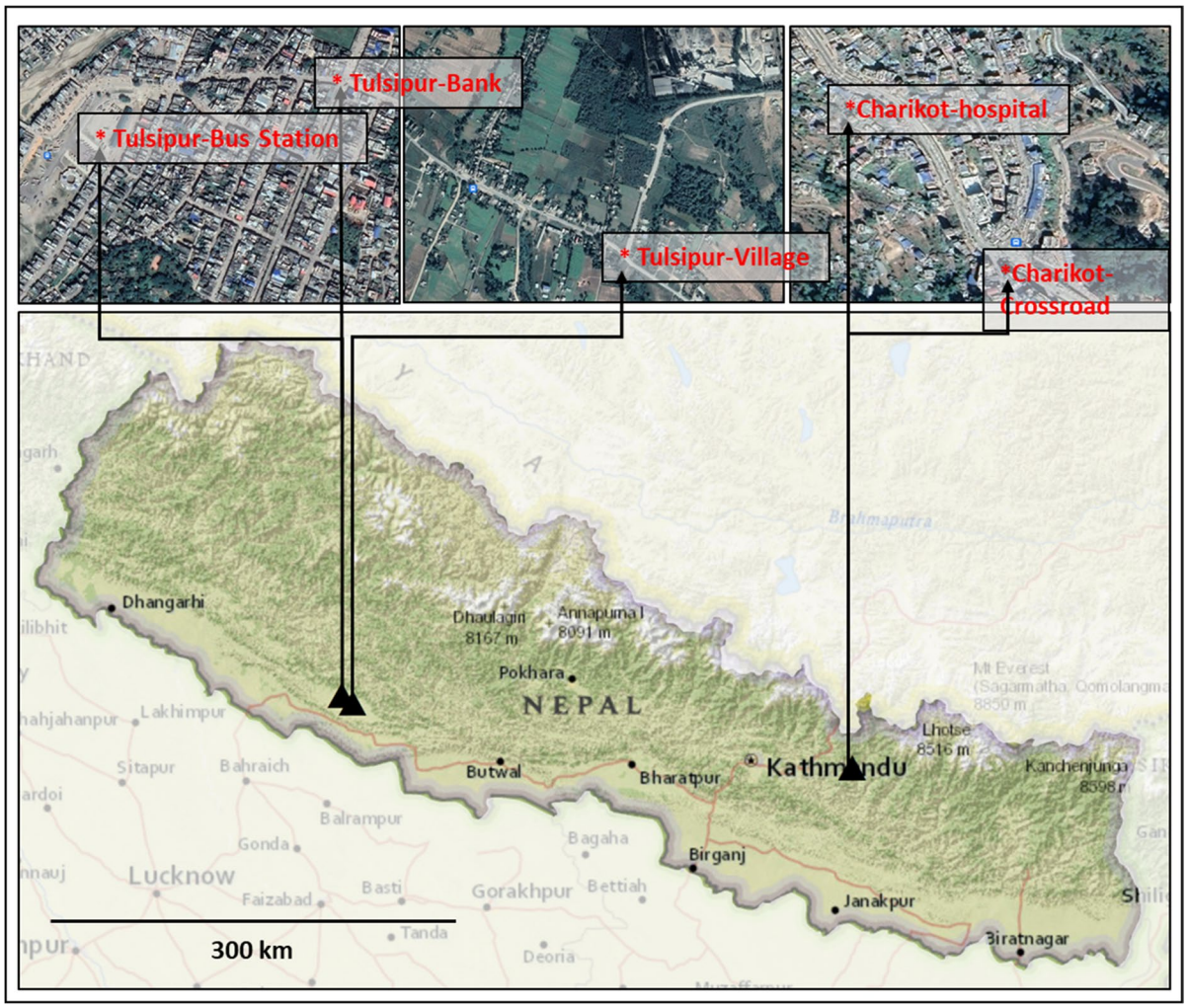

Fig. 1 Monitoring locations in the Nepal cities of Tulsipur and Charikot

The monitoring was conducted in two periods. The first took place in the late August 2018 during the monsoon period finishing and the second in April–May 2019 during the pre-monsoon period. Measurements were conducted at 5 sites, two of which were located in the center of Tulsipur (Tulsipur – Bank 28.133° N, 82.298° E, Tulsipur – Bus Station 28.132°N, 82.292°E), one of which was located in Tulsipur–Village (28.084°N, 82.376°E) (Fig. 1) and two in the center of Charikot, (Charikot – Hospital 27.666°N, 86.046°E Charikot – Crossroad 27.663°N, 86.048°E) (Fig. 1). Tulsipur has increased urbanization and increased numbers of vehicles in recent decades due to increases in the numbers of local residents. It is also a region with significant rural biomass burning. Charikot is located in rural areas of the central Himalayas and is characterized by intense local anthropogenic activities due to increases in the numbers of tourists. In Tulsipur, two polluted locations, near the central bus station and central junction, and one location on the margin of Tulsipur, near cement factory, were selected. In Charikot, two very polluted locations in the city center, a central junction and a hospital, were used. Monitoring took place from 19 to 21 August 2018 (monsoon) and from 30 to 4 May 2019 (pre-monsoon) in Tulsipur and from 26 to 28 August 2018 (monsoon) and from 10 to 13 May 2019 (pre-monsoon) in Charikot. The measurements were performed for 24 h at each location (Central European Summer Time).

2.2 *PM_{10} Concentration and Meteorological Parameter Measurement*

Aerosol in the PM_{10} size fraction was measured using two Haz-Dust EPAM-5000 monitors (Environmental Devices Corporation, USA) equipped with PM_{10} particle size inlets, and during the pre-monsoon period also in parallel with a Cairsens micro-sensor (Envea, France) for particulate matters (PM). The monitor Haz-Dust EPAM-5000 and the Cairsens sensor were placed side by side at a distance of 50 cm. The Haz-Dust EPAM 5000 is a high-sensitivity, real-time monitoring device for particulate matter and is primarily intended for outdoor air quality measurement. This device combines traditional aerosol particle trapping on filters with real-time tracking methods. Haz-Dust EPAM-5000 measures the mass concentration of PM_{10} aerosol particles in the air with a real-time resolution of 1 min based on light scattering from the particles. The data is stored in the device's internal memory and displayed in real time on the device display. The measurement methodology is based on the European Standard for Particulate Measurement in Air (Brunekreef & Maynard, 2008). Particles collected by the Cairsens microsensor pass through a continuous laser beam in the measuring chamber and scatter light in all directions according to the principle of light scattering. This scattered light is analyzed to calculate a mass concentration for the size fraction PM_{10} (Cairsens, 2020). Uncertainty of Haz-Dust EPAM-500 monitor is smaller than 3 μg m^{-3}. Uncertainty of Cairsens micro-sensors is smaller than 5 μg m^{-3}.

Temperature and relative humidity of air were measured with a Young 4137LC/LF sensor (Young Company, Traverse City, Michigan, USA). Wind speed and wind direction were measured with a Gill 2D ultrasonic anemometer (Hampshire, UK), and solar radiation intensity was measured with a RS 81 pyranometer (Envitech Bohemia, Prague, Czech Republic).

2.3 Sampling of Aerosols

Atmospheric aerosols in the size fraction PM_{10} were sampled on quartz fiber (47 mm, QMA, Whatman) and nitrocellulose membrane (47 mm, 1.2 μm porosity, Millipore) filters in parallel at a flow rate of approximately 4 l/min using two aerosol samplers (Haz-Dust EPAM-5000) for 24 h in August 2018 (monsoon period) and May 2019 (pre-monsoon period). The quartz filters were pre-baked at 500 °C for 24 h to remove organic contaminants. Mass concentrations of PM_{10} aerosols were determined gravimetrically from the difference in filter weights before and after sampling using a microbalance (±1 μg, M5P, Sartorius) in a dedicated climate controlled weighing room (48 h, air temperature 20 ± 0.1 °C, relative humidity 50 ± 2%). After weighing, the exposed filters were used for chemical analyzes. A total number of 5 quartz filters in pre-monsoon period (3 in Tulsipur, 2 in Charikot), 5 quartz filters in monsoon period (3 in Tulsipur, 2 in Charikot), and 5 nitrocellulose filters in monsoon period (3 in Tulsipur, 2 in Charikot) were collected.

2.4 Chemical Analysis of Aerosols

2.4.1 Elements

Aerosols collected on nitrocellulose membrane filters were analyzed for elemental content. Each filter was decomposed in 3 mL of concentrated, sub-boil grade nitric acid using a microwave-assisted digestion system (UltraWAVE, Milestone). The decomposed filters were transferred quantitatively along with 7 mL of deionized water into polyethylene scintillation vials (Kartel, Italy). The content of 25 elements (Na, Mg, Al, K, Ca, V, Cr, Mn, Co, Ni, Ti, Cu, Zn, Fe, As, Se, Cd, Sn, Sb, Ba, Tl, Pb, Rh, Pd, and Pt) in the digestions was determined using a triple quadrupole ICP-MS (ICP-MS/MS 8800, Agilent) with two quadrupoles (Q1 and Q2) and an octupole reaction cell in different tune modes (collision/reaction, He, O_2, and NH_3), working in the on mass mode and mass shift mode used to determine selected elements. Cd was analyzed in NH_3 MS/MS mode As, and Se and Fe were analyzed in O_2 MS/MS mode. The forwarded RF power was 1550 W, carrier gas (Ar) flow rate 1.07 L min^{-1}, and integration time per isotope was 0.3 s in all used modes and cell gas flow rates: helium in collision single quadrupole mode: 4 mL min^{-1}, 4^{th} cell gas (O_2 in reaction MS/MS mode): 0.29 mL min^{-1}, 3^{rd} cell gas (NH_3 in reaction MS/MS mode) + helium: 4 mL min^{-1} NH_3 + 1 mL min^{-1} He (Cigánková et al., 2021a).

SRM 1648a Urban Particulate Matter (National Institute of Standards & Technology, Gaithersburg, USA) and ERM-CZ 120 Fine dust (PM_{10}-like) (JRC

European Commission, Belgium) were digested and analyzed at the same conditions as samples for the control of the whole determination process from preparation to determination.

Calibration standards were prepared in a matrix of 2% HNO_3 from a 1.0000 g L^{-1} stock solution of a single element (Analytika Prague, Czech Republic) mixing into one solution in the concentration range of 0–10 mg L^{-1} for Na, Mg, Ca, K, Mn, Al, and Fe and 0 – 100 µg L^{-1} for the rest of elements. Calibration curves of all elements were linear in the whole range ($R^2 = 0.9994–1.0000$). Internal standard for elements determination were prepared from commercial 10 mg L^{-1} mixture of Bi, Ge, In, Li, Sc, Tb, and Y (Agilent technologies, USA) by dilution in 2% HNO_3 to final concentration 100 µg L^{-1}. The tuning solution was prepared from commercial 10 mg.l^{-1} mixture of Li, Co, Y, Ce, Mg, and Tl (Agilent technologies, USA) to final concentration 1 µg L^{-1} each element in a matrix of 2% HNO_3.

The accuracy of the method was periodically evaluated by use of two standard reference materials: SRM 1640a Trace Elements in Natural Water (National Institute of Standards & Technology, Gaithersburg, USA) and SLRS-5 River water reference material for trace elements (National Research Council, Canada). In addition, a control standard (10 µg L^{-1} calibration standard) was measured periodically for instrument stability control. Instrument stability control was online monitored using internal standard solution (Cigánková et al., 2021a).

2.4.2 Organic Compounds

Aerosols sampled on quartz fiber filters were analyzed for polycyclic aromatic hydrocarbons (PAHs) and hopanes content. Recovery standards (phenanthrene-D10, chrysene-D12, perylene-D12, and ααα(20R)-cholestane-D2) were added to the filters prior to organic compounds extraction to compensate for losses during sample preparation. The filters were extracted three times with 15 mL of mixture of a dichloromethane and hexane (*v*/*v* 1:1) for 30 min under ultrasonic agitation. The extracts (total 45 mL) were dried to 0.5 mL under a stream of nitrogen and fractionated by column chromatography (Křůmal et al., 2013). Two fractions were taken after eluting the prepared column with different solvents. The first hexane fraction (30 mL) contained hopanes and the second dichloromethane/hexane fraction (1:1, v/v, 30 mL) contained PAHs. Both fractions were again dried to 1 mL under a gentle stream of nitrogen and analyzed by gas chromatography coupled with mass spectrometry (GC–MS). The GC–MS (Agilent, 7890A, 5975C) was equipped with a capillary column HP5-MS (30 m length, 0.25 mm i.d., and 0.25 µm film thickness). A sample (1 µL) was injected. The carrier gas was helium (5.5) with a flow rate of 1 ml min^{-1}. The MS was operated in electron ionization mode (70 eV) and in single-ion monitoring (SIM) mode with *m/z* characteristic of PAHs, hopanes, and recovery standards (Křůmal et al., 2013).

Analyzed organic compounds included 20 polycyclic aromatic hydrocarbons (i.e., fluorene, phenanthrene, anthracene, fluoranthene, pyrene, retene, benz[a] anthracene, chrysene, triphenylene, benzo[b]fluoranthene, benzo[j]fluoranthene, benzo[k]fluoranthene, benzo[e]pyrene, benzo[a]pyrene, perylene, triphenylbenzene, indeno[1,2,3-c,d]pyrene, dibenz[a,h]anthracene, picene, and benzo[g,h,i]perylene) and 6 hopanes (i.e., 17α,21β-norhopane, 17β,21α-norhopane, 17α,21β-hopane, 17β,21α-hopane, 22S-17α,21β-homohopane, and 22R-17α,21β-homohopane).

Gas Chromatography (GC) Conditions

1. Injection: 1 µL, on-column
2. Temperature program for PAHs: 50 °C, hold for 2 min, gradient from 20 °C-/-min to 150 °C, gradient from 5 °C/min to 300 °C, hold for 15 min
3. Temperature program for hopanes: 50 °C, hold for 2 min, gradient from 10 °C/min to 300 °C, hold for 27 min
4. GC column: HP5-MS, length 30 m, diameter 0.25 mm, stationary phase 0.25 µm
5. Interface temperature: 310 °C

Mass Spectrometry (MS) Conditions

1. Electron ionization, 70 eV
2. Ion source temperature 230 °C, quadrupole temperature 150 °C. Analysis in SIM mode for *m/z* typical for analyzed PAHs (166, 178, 202, 219, 228, 252, 306, 276, 278) and d-PAHs (188, 240, 264)
3. SIM mode analysis for *m/z* typical for analyzed hopanes (191) and ααα(20R)-cholestane-D2 (220)

3 Results and Discussion

3.1 *PM_{10} Concentration and Meteorological Conditions*

Table 1 shows the average temperature and relative humidity of air, global radiation, wind speed, and direction at the measured locations in Tulsipur and Charikot. Daily clocks with zero values were counted when calculating daily average of global radiation. Measurements took place at the studied locations during the pre-monsoon (May) and monsoon (August) seasons, which represent two different types of weather conditions. The monsoon period is mostly accompanied by a higher temperature and higher relative humidity in the studied localities.

The concentrations of PM_{10} aerosol (μg m^{-3}) during the monsoon and pre-monsoon period, measured with a temporal resolution of 30 min using the Haz-Dust monitors at selected locations in Tulsipur and Charikot, are shown in Fig. 2. The concentration of PM_{10} aerosols showed a seasonal trend: in the monsoon season, the daily PM_{10} concentrations were lower than in the pre-monsoon period (Table 2). The lower concentration observed during monsoon season can be attributed to washout by rainfall and higher relative humidity of air leading to reduced resuspension of street dust. In the monsoon period, the 24-h limit value of 50 μg.m^{-3} for human health (World Health Organization, 2006) for PM_{10} was significantly exceeded at the Tulsipur-bus station and Charikor-crossroad (Table 2). On the other hand, during pre-monsoon periods, the WHO limit value for PM_{10} was significantly exceeded at all locations, and the Nepal concentration limit of 150 μg.m^{-3} was exceeded at Tulsipur bus station, Tulsipur village, and Charikot hospital (Table 2). These results are consistent with the minimum PM_{10} level during monsoon period and maximum PM_{10} levels during pre-monsoon periods in Kathmandu Valley in the year 2005 presented by Giri et al., (2004, 2008) who reported the influence of meteorological conditions on PM_{10} concentrations at different locations in the Kathmandu Valley with PM_{10} levels ranging from 7 μg m^{-3} (Matsyagaon) to 633 μg m^{-3} (Putalisadak). Our highest measured 24 h concentration (182.07 μg m^{-3}) at Tulsipur bus station in the pre-monsoon period is about three times lower than the highest daily PM_{10} average of 633 μg m^{-3} in the Kathmandu Valley (Giri et al., 2008).

The PM_{10} concentrations measured in high traffic areas during the present study were mostly much lower values than those reported by Majumder et al. (2012) at a network of ten high-traffic road intersections in the Kathmandu Valley, but similar or lower than those reported in other studies conducted in Nepal (Aryal et al., 2008; Giri et al., 2007, 2008).

PM_{10} concentrations were dynamic during the day, with the minimum at night and the maximum

Table 1 Daily average air temperature, relative air humidity, global radiation, speed, and prevailing wind direction during monsoon and pre-monsoon seasons in Tulsipur and Charikot

Location	Date	Temperature (C°)	Humidity (%)	Global radiation (W m^{-2})	Wind speed (m s^{-1})	Wind direction (deg)
Monsoon						
Tulsipur – bus station	19. – 20. 8. 2018	28	70	135	0.3	west
Tulsipur – bank	20. – 21. 8. 2018	26	80	51	0.6	WNW
Tulsipur – village	21. – 22. 8. 2018	27	83	62	0.2	NW
Charikot – crossroad	26. – 27. 8. 2018	21	86	35	0.3	SSE
Charikot – hospital	28. – 29. 8. 2018	20	87	22	0.3	WNW
Pre-monsoon						
Tulsipur – bus station	1. – 2. 5. 2019	32	63	243	4.3	WNW
Tulsipur – bank	3. – 4. 5. 2019	26	87	201	5.2	E
Tulsipur – village	30. 4. – 1. 5. 2019	32	61	218	5.6	E
Charikot – crossroad	12. – 13. 5. 2019	31	66	219	4.1	S
Charikot – hospital	10. – 11. 5. 2019	32	72	169	5.7	WNW

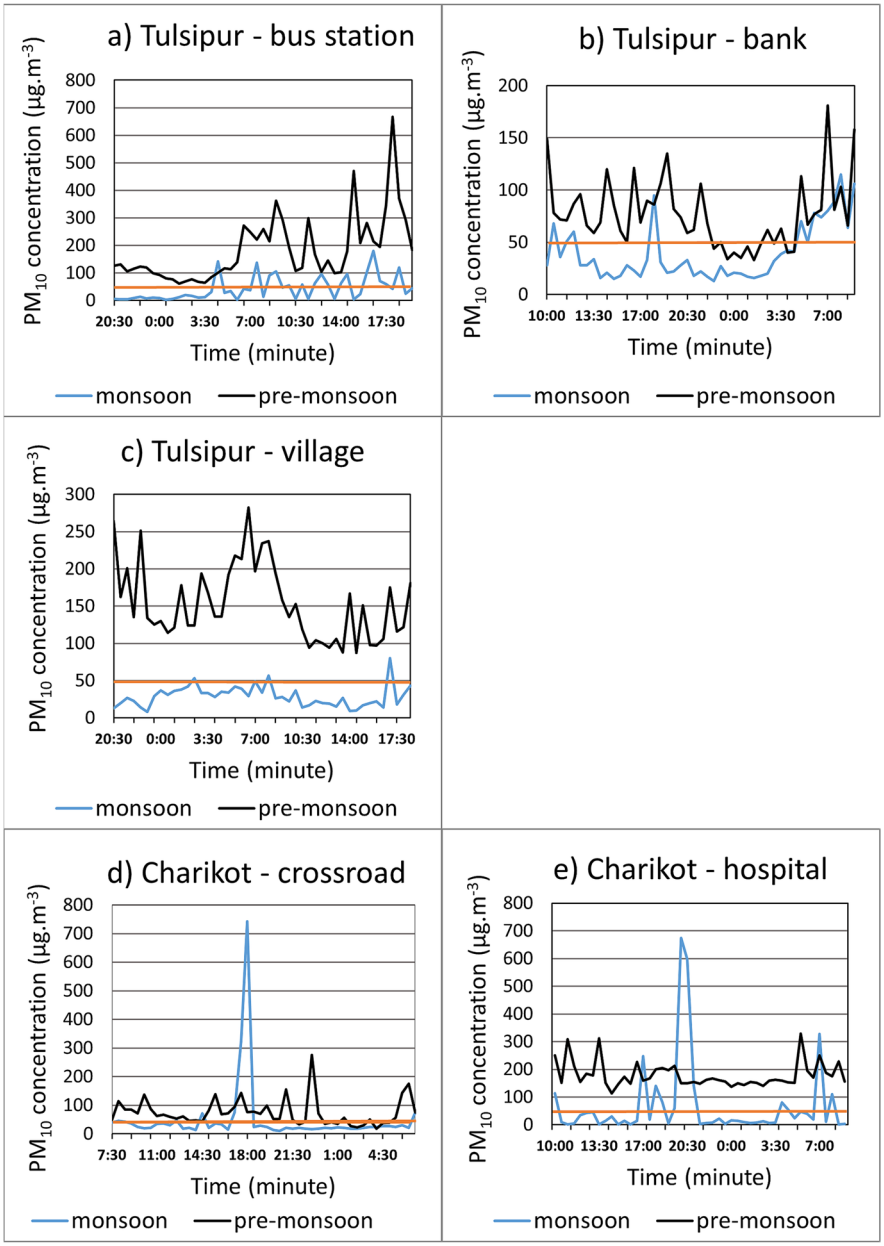

Fig. 2 PM_{10} concentrations (µg m^{-3}) during the monsoon and pre-monsoon period measured with time resolution of 30 min at selected locations in Tulsipur and Charikot. Orange line depicts 24-h PM_{10} limit value of 50 µg $m.^{-3}$ for human health (World Health Organization, 2006)

in the morning and late afternoon at all Tulsipur sites in the pre-monsoon period, as traffic and movement on roads increased at this time (Fig. 2a, b, c). A similar trend was observed in the monsoon period (peak values in the morning and afternoon), but with lower maximum values (Fig. 2a, b, c). The highest PM_{10} concentrations were measured at traffic site at both Tulsipur and Charikot. A very high value (668.34 µg m^{-3}) was measured in the late afternoon at the bus station in Tulsipur (Fig. 2a) in the pre-monsoon season and a concentration of 743.22 µg m^{-3} was measured at a busy crossroad in Charikot (Fig. 2d) at night in the monsoon period and a concentration of 675.43 µg m^{-3} in the late afternoon in Charikot Hospital in the monsoon period (Fig. 2e).

In the monsoon season, the easterly wind direction prevailed in Tulsipur-bus station (Fig. 3a), westerly in

Table 2 Descriptive statistics for daily mean PM_{10} concentration ($\mu g.m^{-3}$) during the monsoon and pre-monsoon period at selected locations in Tulsipur and Charikot measured with Haz-Dust sampler

Statistics	Tulsipur bus station	Tulsipur bank	Tulsipur village	Charikot crossroad	Charikot hospital
Monsoon					
Mean	42.74	39.17	28.81	49.42	69.87
Minimum	6.23	2.44	3.12	3.51	8.24
Maximum	295.25	209.13	119.62	743.22	675.43
Pre-monsoon					
Mean	182.07	77.32	153.67	74.41	180.11
Minimum	61.46	33.13	87.37	18.52	114.13
Maximum	668.34	181.23	283.41	277.22	329.45

Tulsipur-bank (Fig. 3c), northerly in Tulsipur-village (Fig. 3e), and the southerly in Charikot-crossroad (Fig. 3g). Throughout the measurement, the average wind speed in all locations was about 0.6 m s^{-1}, with maximum values up to 0.8 m s^{-1}. In the pre-monsoon period, the variable southwesterly wind direction prevailed in Tulsipur-bus station (Fig. 3b), variable easterly in Tulsipur-bank (Fig. 3d) and Tulsipur-village (Fig. 3f). The variable southeasterly wind direction prevailed in Charikot-crossroad (Fig. 3h) in the pre-monsoon period. The average wind speed was about 4.9 m s^{-1} throughout the measurement at all locations, with peak values up to 9.4 m s^{-1}, which is common for the area during this period (www.meteoblue.com). PM_{10} concentrations correlate with wind direction at each site (Fig. 3).

3.2 *Comparison PM_{10} Results of HAZ-DUST EPAM-5000 Analyzer and Sensor ENVEA PM Cairsens*

The low-cost devices seem to be promising tool for establishing an air quality monitoring network in Nepal, where it is difficult to set up stationary monitoring stations for economic and technical reasons. Due to their small size and low weight, these sensors can also be used for mobile measurements and on unmanned aerial vehicles (drones).

In addition, it is necessary to focus on appropriate methods of data processing (especially their validation) and subsequent interpretation of the results, since the measurement itself can be severely affected not only by the recognized lower accuracy of sensor measurements (Castell et al., 2017) but also by current meteorological conditions (temperature and humidity) or interference from various pollutants (especially observed especially in gaseous sensors) (Lewis et al., 2018).

Figure 4 shows a comparison of measured data from HAZ-DUST EPAM-5000 optical analyzer at a sampling rate of 1 per minute and ENVEA PM Cairsens optical sensor at a sampling rate of 1 per minute at the monitored sites in Tulsipur and Charikot in the pre-monsoon period. The correlation coefficient (R^2) between the raw PM_{10} sensor data and PM_{10} analyzer is 0.96 (RMSE is 63.4 $\mu g\ m^{-3}$) for Tulsipur – bus station (Fig. 4a), 0.94 (RMSE is 42.8 $\mu g\ m^{-3}$) for Tulsipur – bank (Fig. 4b), 0.93 (RMSE is 76.9 $\mu g\ m^{-3}$) for Tulsipur – village (Fig. 4c), 0.84 (RMSE is 51.7 $\mu g\ m^{-3}$) for Charikot – crossroad (Fig. 4d), and 0.85 (RMSE is 54.6 $\mu g\ m^{-3}$) for Charikot – hospital (Fig. 4e). These results indicate a good correlation between the low-cost sensor and the reference analyzer (i.e., Haz-Dust). The accuracy of the optical particle sensor was calculated as the mean error and maximum error compared to the PM_{10} analyzer.

It is evident that the data from both instruments show a similar trend, but they show differences in the particle concentrations measured. This is mainly due to the difference in measurement configuration. PM_{10} concentrations found by Cairsens sensors are in average by 13.2% lower than those found by EPAM analyzer. Sahu et al. (2020) validated Plantower PM sensor measuring ambient PM_{10} concentrations with that measured with optical particle sizers (OPS) and aerodynamic particle sizers (APS) at two sites in the Delhi (India) with Spearman's rank-order correlations (rs = 0.64–0.83) between

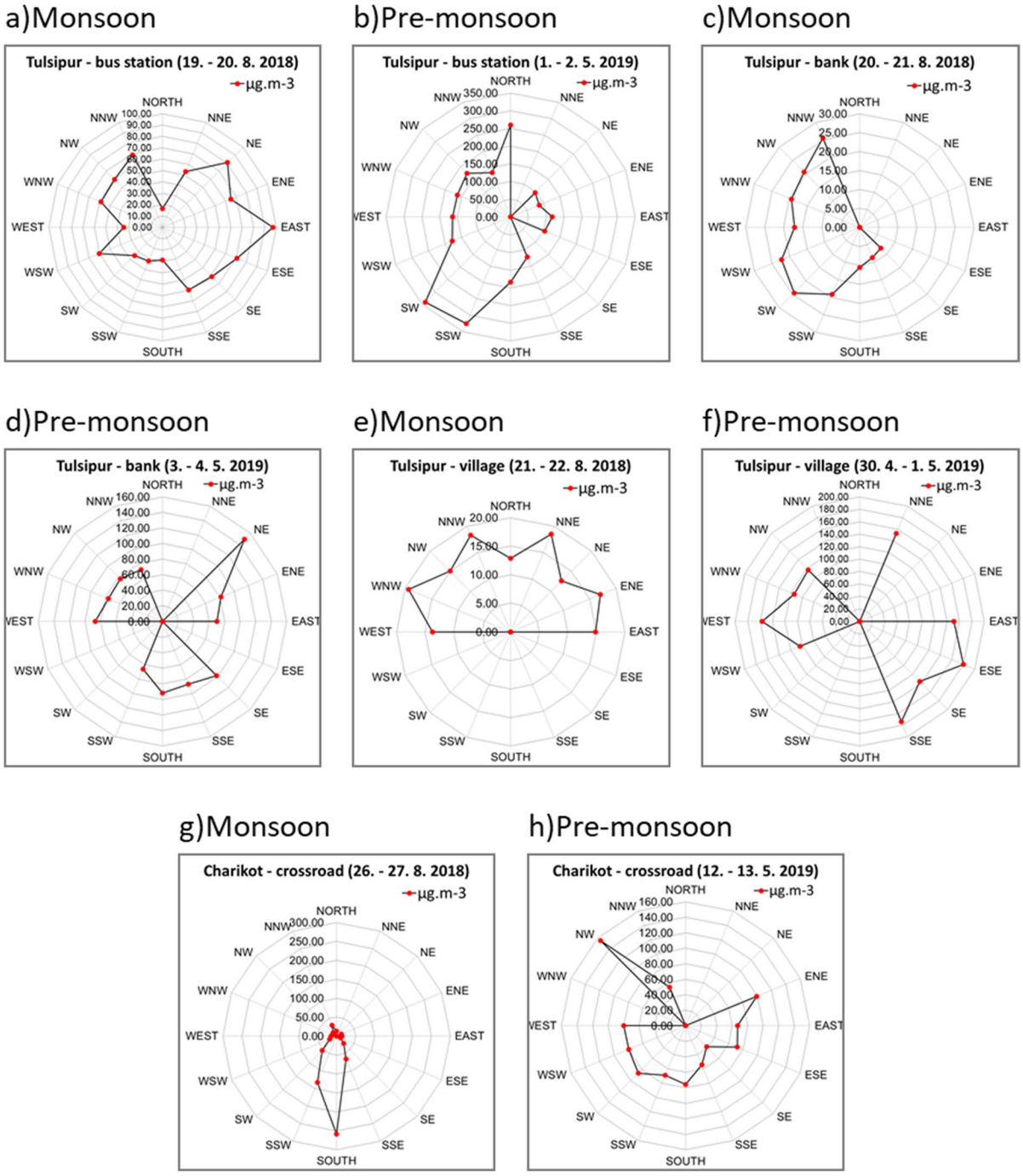

Fig. 3 The wind direction dependence of PM_{10} concentrations for measured locations Tulsipur and Charikot

the studied instruments. Cavaliere et al. (2018) validate low-cost sensor for PM_{10} with an official fixed air quality station at a road site in Florence. For PM_{10} RMSE of 6.1 µg m^{-3}, R^2 0.96 was achieved. However, the low–cost sensor needs to be in detail verified by further experiments and compared with monitors used in automatic airborne PM monitoring network.

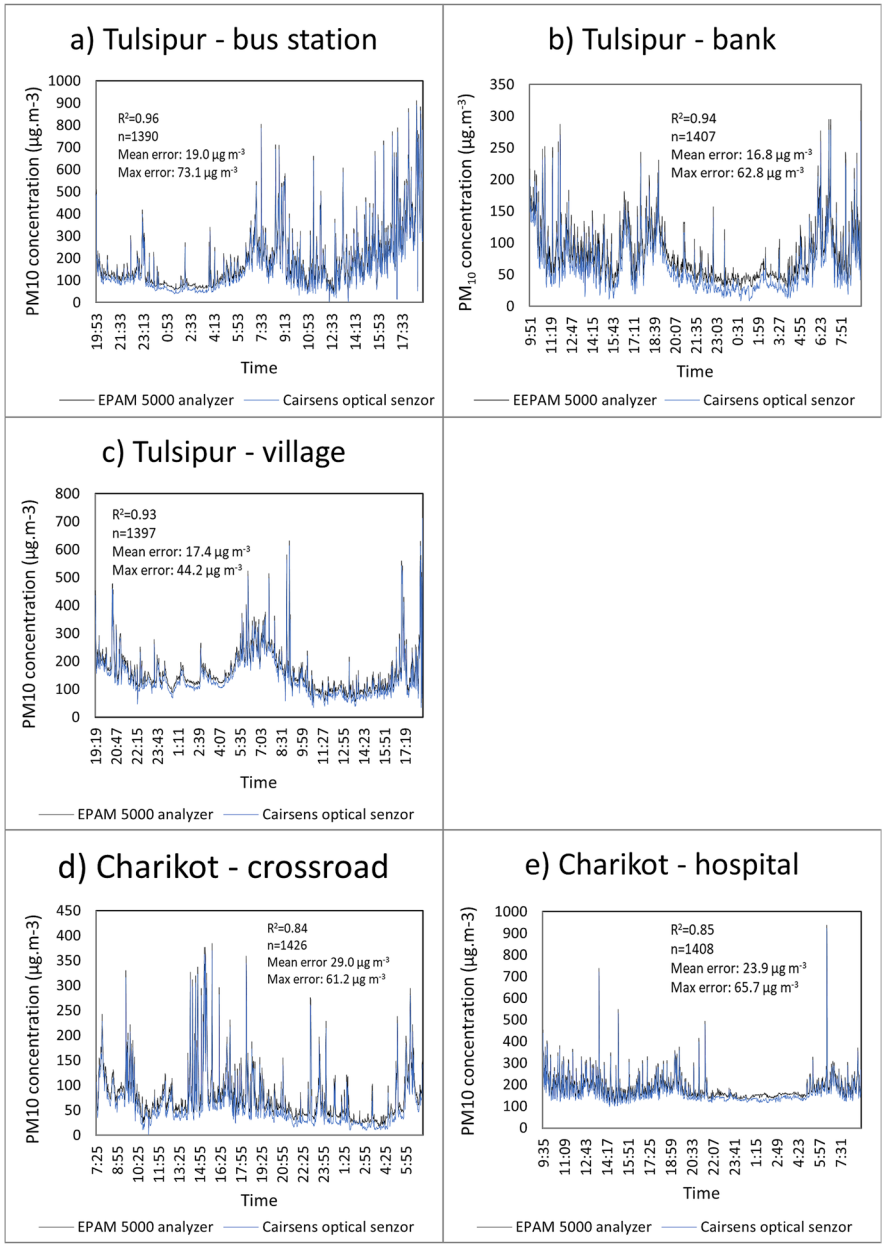

Fig. 4 Comparison of data with time resolution of 1 min from measuring instruments HAZ-DUST EPAM-5000 and ENVEA PM Cairsens in selected locations in Tulsipur and Charikot

3.3 PAHs and Hopanes

All PM_{10} samples were analyzed for PAHs and hopanes. PAHs are generally derived from imperfect combustion of organic matter. Some PAHs serve as a specific molecular markers for the combustion of plastics (1,3,5-triphenylbenzene), softwood (retene), or coal (picene). Gasoline vehicles emit higher concentrations of indeno[1,2,3-c,d]pyrene, dibenz[a,h]anthracene and benzo[g,h,i]perylene, while diesel vehicles emit higher concentrations of phenanthrene and pyrene (Mikuška et al., 2015; Ravindra et al., 2008; Simoneit et al., 2005). PAHs were present in low concentrations in all PM_{10} samples (Table 3). Low-molecular weight PAHs (naphthalene, acenaphthylene, and acenaphthene) resulted in high losses during sample preparation; therefore, these PAHs were not quantified. Phenanthrene/anthracene, benz[a]anthracene/chrysene/triphenylene, and benzo[b+j+k]fluoranthene are listed in the table as sum values because these compounds were not sufficiently separated in the GC column.

Table 3 Concentration and LOD of PAHs analyzed (ng m^{-3}) in PM_{10} aerosol during the monsoon (M) and pre-monsoon (P-M) period at selected locations in Tulsipur and Charikot

	Tulsipur bus station		Tulsipur bank		Tulsipur village		Charikot crossroad		Charikot hospital		LOD	
	M	P-M	M	P-M	M	P-M	M	P-M	M	P-M	M	P-M
Fluorene (Flu)	0.182	< LOD	0.234	< LOD	0.207	< LOD	0.524	< LOD	0.215	< LOD	0.101	0.187
Phenanthrene (Phe) + anthracene (Ant)	< LOD	0.333	0.055	< LOD	< LOD	0.211	0.043	0.301	0.059	0.463	0.0397	0.058
Fluoranthene (Fla)	0.044	0.082	0.084	< LOD	< LOD	0.412	0.061	0.185	< LOD	0.338	0.039	0.0555
Pyrene (Pyr)	0.096	0.184	0.081	0.0669	< LOD	0.516	0.105	0.311	0.088	0.519	0.0377	0.0529
Retene	< LOD	0.1295	< LOD	0.1104	< LOD	0.2602	< LOD	0.831	< LOD	0.316	0.6	0.111
Benz[a]anthracene (BaA) + chrysene (Chr) + triphenylene	0.088	0.159	0.122	0.132	< LOD	0.716	0.116	0.9501	0.123	0.575	0.063	0.105
Benzo[b + j + k]fluoranthene (BkjkF)	0.21	0.185	0.156	0.161	0.0675	0.553	0.122	0.262	0.149	0.237	0.0266	0.0413
Benzo[e]pyrene (BeP)	0.365	0.871	0.189	0.344	0.121	2.595	0.233	0.378	0.209	0.455	0.102	0.0392
Benzo[a]pyrene (Bap)	0.145	1.35	0.122	0.494	< LOD	3.53	0.123	0.531	0.153	0.706	0.0808	0.125
Perylene	0.096	1.056	0.219	0.321	< LOD	3.22	< LOD	0.379	0.142	0.577	0.0766	0.1301
1,3,5-triphenylbenzene	< LOD	1.168	< LOD	0.152	< LOD	3.45	< LOD	0.239	< LOD	0.302	0.121	0.112
Indeno[1,2,3-c,d]pyrene (IndP)	0.686	1.49	1.28	0.877	< LOD	4.55	0.388	1.57	0.422	0.369	0.195	0.087
Dibenz[a,h]anthracene (DahA)	< LOD	8.75	0.281	< LOD	< LOD	15.05	< LOD	3.62	< LOD	2.12	0.118	0.125
Picene	< LOD	8.059	0.532	< LOD	< LOD	12.9	< LOD	3.21	< LOD	1.24	0.148	0.119
Benzo[g,h,i]perylene (BghiP)	0.568	7.89	0.995	< LOD	< LOD	12.4	0.395	3.39	0.381	< LOD	0.101	0.167
Σ PAHs	2.48	31.7	4.35	2.65	0.396	60.4	2.11	16.2	1.94	8.22		

Indeno[1,2,3-c,d]pyrene, dibenz[a,h]anthracene, and benzo[g,h,i]perylene were the most abundant PAHs both at Tulsipur and Charikot, while lighter PAHs such as phenanthrene, fluoranthene, or pyrene were present at lower concentrations.

The measured PAH concentrations were different at the five sampling sites in both the monsoon and pre-monsoon period. In addition, the concentration of PAHs showed seasonal variation with concentrations higher in the pre-monsoon period than in the monsoon period at all sites (except the Tulsipur bank at a busy traffic junction). The mean total PAH concentrations during the monsoon period were 2.4 ng m^{-3} in Tulsipur and 2.0 ng m^{-3} in Charikot in the monsoon period and 31.6 ng m^{-3} in Tulsipur and 12.2 ng m^{-3} in Charikot in pre-monsoon period, respectively. Concentrations during the monsoon period were similar at both locations, but during pre-monsoon period, PAH concentrations were higher in Tulsipur than Charikot. A similar difference between the southern rural area of Nepal (Tulsipur) and the Northern Himalayan region of Nepal (Charikot) was recently found in another study (Chen et al., 2017).

Table 4 compares our results for PAHs with other Nepalese and foreign cities in Asia. The average values of PAHs for each location listed in the table did not differ between monsoon and pre-monsoon periods, except for Nanjing (urban district) in China and Barapani (foothills of Himalayas) in the Nepal in pre-monsoon season. The values at Tulsipur Bank (2.7 ng m^{-3}), Charikot crossroad (16.2 ng m^{-3}), and Charikot Hospital (8.2 ng m^{-3}) in the pre-monsoon season are lower to those reported (Wang et al., 2017) in Nanjing (18.1 ng m^{-3}) in China and higher (except Charikot junction) than the value reported (Rajput et al., 2013) in Barapani (14.1 ng m^{-3}) in Nepal in the pre-monsoon season.

Hopanes, which serve as coal combustion and traffic markers, were found in PM_{10} samples only in the pre-monsoon period (Table 5). The concentrations

Table 4 The concentrations (ng m^{-3}) of PAHs analyzed in PM_{10} aerosol in different cities of Nepal and their comparison with other cities in Asia

Location	Characterization of site	Number of PAHs	Mean concentration	Sample period	Reference
Tulsipur bus station		17	2.5	19 August 2018	This study
Tulsipur bank		17	4.3	20 August 2018	This study
Tulsipur village		17	0.4	21 August 2018	This study
Charikot crossroad		17	2.1	26 August 2018	This study
Charikot hospital		17	1.9	28 August 2018	This study
Tulsipur bus station		17	31.7	30 April 2019	This study
Tulsipur bank		17	2.7	1 May 2019	This study
Tulsipur village		17	60.4	3 May 2019	This study
Charikot crossroad		17	16.2	10 May 2019	This study
Charikot hospital		17	8.2	12 May 2019	This study
Kathmandu, Nepal	The capital city	15	3.1	2012	Pokhrel et al., 2018
Kathmandu, Nepal		15	16.1	August 2014-August 2015	Pokhrel et al., 2018
Pokhara, Nepal	Rural areas in central Himalaya	15	14.1	August 2014-August 2016	Pokhrel et al., 2018
Hetauda, Nepal	Agricultural-rural	15	11.1	November 2015-August 2016	Pokhrel et al., 2018
Lumbini, Nepal	Agricultural-rural	15	91.6	April 2013-March 2014	Chen et al., 2017
Pokhara, Nepal		15	20.7	April 2013-March 2014	Chen et al., 2017
Dhunche, Nepal	Semi-urban town in Himalayas	15	18.6	April 2013-March 2014	Chen et al., 2017
Jomsom, Nepal	Rural areas in central Himalaya	15	11.1	April 2013-March 2014	Chen et al., 2017
Barapani, Nepal	Foothills of the Himalayas		14,1	January 2010-March 2010	Rajput et al, 2013
Nanjing, China	Urban district	16	18.1	April- May, 2015	Wang et al., 2017
Zhongba, China	Tibet-Himalayas	15	8.8	April 2013-March 2014	Chen et al., 2017
Agra, India	Industrial area	16	72.7	May 2006-December 2009	Lakhani, 2012

of some hopanes in the samples were slightly above the limit of detection (LOD) and were affected by the higher uncertainty of analytical determination, while the concentrations of hopanes in all monsoon samples were below LOD (0.080—0.302 ng/m^3). The mean total concentration of hopanes during the pre-monsoon period was 1.39 ng m^{-3} in Tulsipur and 0.69 ng m^{-3} in Charikot. At both sites, the highest concentrations were found for 17α(H),21β(H)-norhopane that serves as a tracer for motor vehicle exhaust (Mikuška et al., 2015). The high concentrations were found also for 17α(H),21β(H)-hopane, another marker of traffic.

Since the concentrations of hopanes in the air have not yet been measured in Nepal, we compared our results with urban and mountain measurements in China (Table 6). The concentrations of selected hopanes in Tulsipur and Charikot were several times lower than those in Baoji (urban). On the other hand, the concentration of 17α,21β-hopane in Tulsipur and Charikot was 2–5 times higher than that in Mt. Tai (mountain) and the concentration of 17α,21β-norhopane was 5–14 times higher than that in Mt. Tai (mountain).

3.4 Elements

25 elements were analyzed in PM_{10} samples collected only during monsoon period due to a failure of one sampler during the 1st day of sampling in the pre-monsoon period. The concentration of platinum elements (Rh, Pd, and Pt) in all samples was below the value of LOD. The concentrations of the other analyzed elements in PM_{10} are shown in Table 7 and Fig. 5. Al was dominant element followed by Ca, Fe, K, Mg, Na, and Ti in all locations except Tulsipur – village. High concentrations of these elements (Fe, Ca, Al, Mg, Na, K, and Ti) were mainly due to street dust resuspension of Earth crust material by wind or vehicle operation. Other elements were present in PM_{10} aerosol samples at lower concentrations. The sum of elements in localities in Tulsipur town (15.1,

Table 5 Concentrations and LOD of hopanes (ng m^{-3}) analyzed in PM_{10} aerosol during the pre-monsoon period at selected locations in Tulsipur and Charikot

	Tulsipur bus station	Tulsipur bank	Tulsipur village	Charikot crossroad	Charikot hospital	LOD
17α,21β-norhopane	0.7725	0.47	0.46	0.25	0.32	0.09
17β,21α-norhopane	< LOD	< LOD	< LOD	< LOD	< LOD	0.09
17α,21β-hopane	0.58	0.44	0.31	0.22	0.26	0.10
17β,21α-hopane	< LOD	< LOD	< LOD	< LOD	< LOD	0.10
22S-17α,21β-homohopane	0.35	0.26	< LOD	< LOD	0.16	0.14
22R-17α,21β-homohopane	0.31	0.22	< LOD	< LOD	0.18	0.16
Σ hopanes	2.02	1.39	0.77	0.46	0.92	

Table 6 The concentrations (ng m^{-3}) of hopanes PM_{10} aerosol in Tulsipur and Charikot and their comparison with urban and mountain locality in China

	Sample period	17α,21β-norhopane	17β,21α-norhopane	17α,21β-hopane	17β,21α-hopane	Reference
Tulsipur bus station	30 April 2019	0.77	< LOD	0.58	< LOD	This study
Tulsipur bank	1 May 2019	0.47	< LOD	0.44	< LOD	This study
Tulsipur village	3 May 2019	0.46	< LOD	0.31	< LOD	This study
Charikot crossroad	10 May 2019	0.25	< LOD	0.22	< LOD	This study
Charikot hospital	12 May 2019	0.32	< LOD	0.26	< LOD	This study
Baoji (urban) China	Spring (4 days)	10.0	13.0	6.83	7.74	Wang et al., 2009
Mt. Tai (mountain) China	Spring (7 days)	0.05	< LOD	0.11	< LOD	Wang et al., 2009

Table 7 Concentration of analyzed elements (ng m^{-3}) in PM_{10} aerosol at selected locations in Tulsipur and Charikot during the monsoon period

Elements	Tulsipur bus station	Tulsipur bank	Tulsipur village	Charikot crossroad	Charikot hospital
Na	329	169	105	115	164
Mg	1400	559	238	190	308
Al	4442	1722	358	917	1783
K	2100	876	431	579	1025
Ca	3758	1688	2069	779	1079
Ti	107	60.70	16	39.80	77.20
Fe	2813	1200	353	607	1014
V	5.69	2.60	0.63	0.79	1.58
Cr	4.22	1.13	3.67	12.60	18.80
Mn	66.50	28	5.83	9.49	17.60
Co	1.56	0.39	0.13	0.22	0.36
Ni	2.04	0.44	1.85	0.26	0.59
Cu	2.33	6.61	˂LOD	˂LOD	˂LOD
Zn	23.60	19.80	11.80	17.60	15.10
As	1.13	0.63	0.25	0.18	0.22
Se	0.20	0.13	0.18	0.02	0.11
Cd	0.15	0.26	0.08	2.80	0.15
Sn	14.90	3.95	2.48	2.40	2.02
Sb	0.26	0.19	0.05	0.16	0.03
Ba	38.6	16.5	2.11	5.36	9.62
Tl	0.06	0.04	1.40	0.05	0.05
Pb	5.67	3.67	2.99	1.58	1.01
Σ elements (μg m^{-3})	15.1	6.36	3.60	3.28	5.52

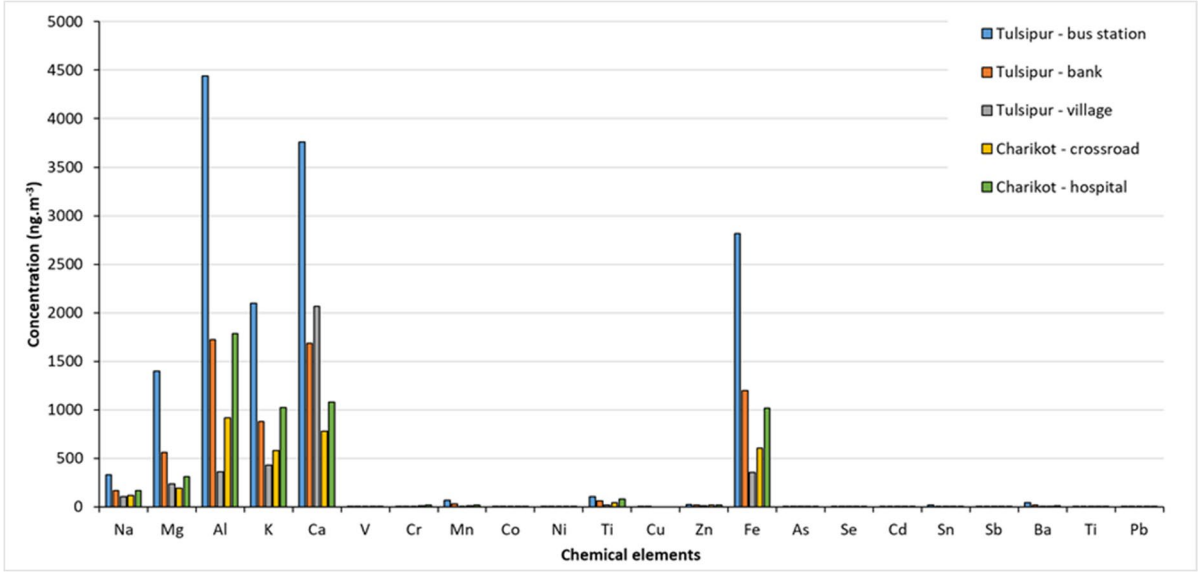

Fig. 5 Comparison of concentrations of elements in PM_{10} aerosol at selected locations in Tulsipur and Charikot during the monsoon period

6.36 and 3.60 ng m^{-3}) is mostly higher than those in localities in Charikot (3.28 ng m^{-3}, 5.52 ng m^{-3}). The sum of elements in localities in Tulsipur village (3.60 ng m^{-3}) is similar to Charikot crossroad (3.28 ng m^{-3}).

Table 8 compares our results with selected foreign localities. The concentrations of elements in Tulsipur and Charikot were higher than those reported by Tyagi et al. (2012) for rural and industrial sites in India except Cr at Tulsipur – bank. On the contrary, the concentrations of elements in localities in India are lower compared to Tulsipur and Charikot.

3.5 Source Identification

Identification of emission sources of analyzed aerosols and their components is currently mostly performed by using various multivariate receptor models (Cigánková et al., 2021a; Mikuška et al., 2020; Viana et al., 2008). However, the use of receptor models is not possible in this study due to the small number of PM_{10} samples. Therefore, the emission sources of the analyzed PM_{10} aerosols were identified using the diagnostic ratios and the content of selected organic markers and elements in the analyzed samples (Cigánková et al., 2021a; Křůmal et al., 2013, 2017; Mikuška et al., 2015, 2020).

The presence of retene and picene in PM_{10} samples proves the combustion of biomass and coal (Křůmal et al., 2017; Mikuška et al., 2015) as the sources of PAHs in analyzed PM_{10} samples, while the presence of 1,3,5-triphenylbenzene suggests the combustions of plastics and waste (Simoneit et al., 2005). The high concentration of indeno[123-*cd*] pyrene, dibenz[a,h] anthracene, and benzo[*g,h,i*]perylene in the PM_{10} samples indicates vehicular emissions (particularly emissions from gasoline vehicles) as another emission source of the PM_{10} aerosols in Tulsipur and Charikot (Mikuška et al., 2015; Ravindra et al., 2008).

Presence of hopanes in PM_{10} aerosol samples indicates both traffic and coal combustion as emission source of hopanes in both Tulsipur and Charikot. 17α(H),21β(H)-norhopane was the most abundant hopane, which together with high concentration of 17α(H),21β(H)-hopane and similar concentrations of *R* and *S* isomer of 17α(H),21β(H)-homohopane proves that hopanes in Tulsipur and Charikot originated predominantly from traffic emissions.

Table 8 The concentrations (ng m^{-3}) of elements in PM_{10} aerosol in Tulsipur and Charikot and their comparison with other localities in Asia

Location	Elements									Sample period	Reference
	Cu	Zn	Pb	Cr	Ni	Fe	Cd	Mn	Al		
Tulsipur bus station	2.33	23.60	5.67	4.22	2.04	2813	0.15	66.50	4442	19 August 2018	This study
Tulsipur bank	6.61	19.80	3.67	1.13	0.44	1200	0.26	28.0	1722	20 August 2018	This study
Tulsipur village	ʿLOD	11.80	2.99	3.67	1.85	353	0.08	5.83	358	21 August 2018	This study
Charikot crossroad	ʿLOD	17.60	1.58	12.60	0.26	607	2.80	9.49	917	26 August 2018	This study
Charikot Hospital	ʿLOD	15.10	1.01	18.8	0.59	1014	0.15	17.60	1783	28 August 2018	This study
Chak (rural site), Pakistan	0.56	1.36	9.32		151		35.10	0.98	7.21	August-November 2007, June 2008	Nasir et al., 2015
Bhaun (rural site), Pakistan	0.27	1.01	9.53		31.9		79.20	0.62	7.87	August-November 2007, June 2008	Nasir et al., 2015
Lahore (urban site), Pakistan	0.30	0.85	16.20		65.80		31.70	0.34	3.01	August-November 2007, June 2008	Nasir et al., 2015
Roorkee (industrial site), India	0.37				0.28		0.02			January-March 2007	Tyagi et al., 2012
Molna (rural site), India		7.13		2.04		30		0.80	15.60	January-March 2007	Tyagi et al., 2012
Wah Cantt (industrial site), Pakistan		3.94	137								Nazir et al., 2011

The parental PAH ratios are calculated to identify the origin of PAHs (Rajput et al., 2014). Table 9 lists most commonly used parental PAH ratios (Rajput et al., 2014) calculated for aerosols collected during the monsoon and pre-monsoon period at selected sites in Tulsipur and Charikot and their comparison with other sites in Nepal and China. In this case, they are indeno[1,2,3-cd]pyrene, benzo[g,h,i]perylene, fluoranthene, and pyrene. If the ratio IndP / (IndP + BghiP) is less than 0.2, it is unprocessed oil, if it is between 0.2 and 0.5, it is petroleum products combustion and the value more than 0.5 shows biomass and coal combustion. For the ration Fla / (Fla + Pyr), it is less than 0.4, it is clear that it is crude oil, if it is between 0.4 and 0.5, it is the combustion of petroleum products and the combustion of biomass and coal shows values more than 0.5 (Chen et al., 2017; Yunker et al., 2002).

Table 9 shows the diagnostic ratios of PAHs in aerosols during the monsoon and pre-monsoon period at selected sites in Tulsipur and Charikot and their comparison with other sites in Nepal and China. From the measurements, it is clear that the average IndP / (IndP + BghiP) ratio was higher than 0.5 during the measurements in the monsoon period at individual locations in Tulsipur and Charikot, which clearly indicates high pollution from biomass and coal burning. In pre-monsoon period, the ratio was less than 0.5, suggesting combustion of petroleum products probably within vehicle traffic or household activities as a source of PAHs. For the Fla / (Fla + Pyr) ratio, values between 0.3 and 0.5 prevailed, indicating a high proportion of combustion of petroleum products.

A ratio of B*e*P/(B*e*P + B*a*P) due to different atmospheric stability of both species is frequently used to distinguish local/regional sources from long range transport of pollutants (Mikuška 2015). In pre-monsoon period, the values of the ratio for both studied localities were smaller than 0.5 (mean value of 0.41), which indicates sampling of PM_{10} aerosols freshly emitted from the local or nearby regional emission sources. During monsoon period, the values of the ratio for both studied localities were higher than 0.5 (mean value of 0.64), suggesting transport of sampled PM_{10} aerosols from larger distances.

The elements analyzed in collected PM_{10} aerosols largely originate from various emission sources such as resuspension of Earth crust material (Al, Ca, Mg, Fe, Ti, K, etc.), industrial activity (Fe, Co, Cd, Cu, Cr, V, Ni, As, Ca, Mn, Sn, Zn, etc.), biomass (wood) burning (K, Mn, Cu, Pb, Zn, Na, etc.), coal combustion (Se, As, Cd, K, Mn, Zn, Pb, Na, Cu, Ca, Tl, Cr, etc.), emissions from automobile transport (Sb, Mn, Ba, Zn, Cu, Fe, V, Ca, Tl, Sn, Cd, Cr, Mg, Ni, and Pb), oil combustion (V and Ni), cement plant (Ca, Zn, Fe, Mn, Sb, Pb, Cd, Tl, As, Cu, Ni, etc.), and others.

Table 9 Diagnostic ratios of PAHs in aerosols during the monsoon and pre-monsoon period at selected locations in Tulsipur and Charikot and their comparison with other localities in Nepal and China

Sample period	Pre-monsoon	Monsoon	Pre-monsoon	Monsoon	Reference
Diagnostic ratio of PAHs	IndP/(IndP + BghiP)	IndP/(IndP + BghiP)	Fla/(Fla + Pyr)	Fla/(Fla + Pyr)	
Tulsipur village	0.27	*	0.44	*	This study
Tulsipur bus station	0.16	0.55	0.31	0.31	This study
Tulsipur bank	*	0.56	*	0.51	This study
Charikot crossroad	0.32	0.50	0.37	0.37	This study
Charikot Hospital	*	0.53	0.39	*	This study
Lumbini, Nepal	0.57	0.53	0.49	0.48	Chen et al., 2017
Pokhara (rural areas in central Himalayas, Nepal, Nepal	0.75	0.60	0.38	0.42	Chen et al., 2017
Jomson (rural areas in central Himalayas, Nepal	0.45	0.43	0.47	0.46	Chen et al., 2017
Dhunche, Nepal	0.52	0.54	0.48	0.48	Chen et al., 2017
Zhongba (Tibet-Himalayas), China	0.42	0.42	0.48	0.47	Chen et al., 2017
Nyalam (Tibet-Himalayas), China	0.45	0.43	0.48	0.47	Chen et al., 2017
Nanjing (urban district), China	0.49	-	0.40	-	Wang et al., 2017

*Not calculated due to PAH concentration < LOD

Precise identification of the emission source of a particular elements is difficult because of the overlap of the individual emission sources (Mikuška et al., 2020; Tasić et al, 2017). However, some elements serve as markers of a certain emission source, e.g., potassium is considered as a good marker for biomass burning, while Se, As, and Cd indicate coal combustion and Ni and V combustion of oil. Sb, Ba, Zn, Cu, Mn, Tl, and Fe are important markers of traffic emissions. Increased concentration of thallium in PM_{10} sampled in Tulsipur village could indicate combustion of coal or production of cement in the cement factory located north of Tulsipur (Karbowska, 2016).

From the above, it is clear that the combustion of biomass (predominantly wood) and coal combined with the dense traffic and street dust resuspension is the main reasons of air pollution in the measured localities in Tulsipur and Charikot. In addition, the incineration of waste in households is another possible source of elements and PAHs. The cement factory located nearby Tulsipur also contributes to the composition of PM_{10} aerosols in Tulsipur.

4 Conclusion

In this study, PAHs, hopanes, and elements were analyzed in PM_{10} aerosols collected in Tulsipur and Charikot in Nepal in monsoon and pre-monsoon period. The PM_{10} aerosols and their components were analyzed for the first time in these Nepalese cities. In addition, the concentrations of hopanes and elements in PM_{10} aerosols have not yet been measured in Nepal.

The WHO 24-h limit value of 50 μg m^{-3} and the Nepal concentration limit of 150 μg m^{-3} for human health for PM_{10} was significantly exceeded in the pre-monsoon periods. The concentrations of PM_{10} and analyzed organic components (i.e., PAHs and hopanes) showed seasonal variations in both Tulsipur and Charikot, with lower concentrations in monsoon period and the higher values in pre-monsoon period. The lower concentration observed during monsoon season can be attributed to washout by rainfall of aerosols and higher relative humidity of air leading to reduced resuspension of street dust.

Traffic, biomass (mainly wood) burning, and coal combustion were identified as prevailing local sources of PAHs and several elements analyzed in PM_{10} aerosols sampled in Tulsipur and Charikot. The incineration of waste in households was suggested as another source of elements and PAHs. Aluminum and other elements of Earth crust material in PM_{10} aerosol samples originate predominantly from street dust resuspension. Calcium, thallium, and other elements found in Tulsipur samples may be emitted by the cement factory located nearby Tulsipur. The traffic was suggested as the prevailing emission source of hopanes in Tulsipur and Charikot.

The value of diagnostic ratio IndP/(IndP + BghiP) during post-monsoon period indicates pollution due to combustion of biomass and coal, while during pre-monsoon period indicates pollution due to petroleum combustion. The ratio Fla / (Fla + Pyr) indicates petroleum product combustion during both pre-monsoon and monsoon period.

The diagnostic ratio BaP/(BeP + BaP) indicates emission of PM_{10} aerosols prevaily from the local or nearby regional emission sources in pre-monsoon period, while during monsoon period, the ratio for both studied localities suggests transport of sampled PM_{10} aerosols from larger distances.

Acknowledgements This research was supported by the Grant Agency of the Czech Republic under the project No. 503/20/02203S.

Data Availability The datasets generated during and/or analyzed during the current study are available from the corresponding author on reasonable request.

Declarations

Conflict of Interest The authors declare no competing interests.

References

Adhikary, B., Carmichael, G.R., Tang, Y., Leung, L.R., Qian, Y., Schauer, J.J., Stone, E.A.,

Aryal, R. K., Lee, B. K., Karki, R., Gurung, A., Kandasamy, J., Pathak, B. K., Sharma, S., & Giri, N. (2008). Seasonal PM10 dynamics in Kathmandu Valley. *Atmospheric Environment, 42*(37), 8623–8633. https://doi.org/10.1016/j.atmosenv.2008.08.016

Bhargava, A., Khanna, R., Bhargava, S., & Kumar, S. (2004). Exposure risk to carcinogenic PAHs in indoorair during biomass combustion whilst cooking in rural India. *Atmospheric Environment, 38*(28), 4761–4767. https://doi.org/10.1016/j.atmosenv.2004.05.012

Biswas, K., Chatterjee, A., Chakraborty, J. (2020). Comparison of air pollutants between Kolkata and Siliguri, India, and its relationship to temperature change. Journal of Geovisualization and Spatial Analysis, 4(25). https://doi.org/10.1007/s41651-020-00065-4.

Brunekreef, B. Holgate, S.T. Air pollution and health (2002). The Lancet, 360(9341), 1233–1242. https://doi.org/10.1016/S0140-6736(02)11274-8.

Bonasoni, P., Laj, P., Marinoni, A., Sprenger, M., Angelini, F., Arduini, J., Bonafe, U., Calzolari, F., Colombo, T., Decesari, S., Di Biagio, C., Di Sarra, A., Evangelisti, F., Duchi, R., Facchini, M., Fuzzi, S., Gobbi, G., Maione, M., Panday, A., … Cristofanelli, P. (2010). Atmospheric brown clouds in the Himalayas: First two years of continuous observations at the Nepal Climate Observatory-Pyramid (5079 m). *Atmospheric Chemistry and Physics, 10*, 7515–7531. https://doi.org/10.5194/acp-10-7515-2010

Brunekreef, B., & Maynard, R. L. (2008). A note on the 2008 EU standards for particulate matter. *Atmospheric Environment, 42*(26), 6425–6430. https://doi.org/10.1016/j.atmosenv.2008.04.036

Cairsens (2020). Cairsens PM microsensors. Technical Manual. ENVEA. Retrieved July 2021 from www.envea.global.

Castell, N., Dauge, F. R., Schneider, P., Vogt, M., Lerner, U., Fishbain, B., et al. (2017). Can commercial low-cost sensor platforms contribute to air quality monitoring and exposure estimates? *Environment International, 99*, 293–302. https://doi.org/10.1016/j.envint.2016.12.007

Cavaliere, A., Carotenuto, F., Di Gennaro, F., Gioli, B., Gualtieri, G., Martelli, F., Alessandro Matese, A., Toscano, P., Vagnoli, C., & Zaldei, A. (2018). Development of low-cost air quality stations for next generation monitoring networks: calibration and validation of PM2.5 and PM10 sensors. *Sensors, 18*(9), 2843. https://doi.org/10.3390/s18092843

Chen, P., Kang, S., Li, C., Rupakheti, M., Yan, F., Li, Q., Ji, Z., Zhang, Q., Luo, W., & Sillanpää, M. (2015). Characteristics and sources of polycyclic aromatic hydrocarbons in atmospheric aerosols in the Kathmandu Valley. *Nepal. Science of the Total Environment, 538*, 86–92. https://doi.org/10.1016/j.scitotenv.2015.08.006

Chen, P., Li, C., Kang, S., Rupakheti, M., Panday, A. K., Yan, F., Li, Q., Zhang, Q., Guo, J., Ji, Z., Rupakheti, D., & Luo, W. (2017). Characteristics of particulate-phase polycyclic aromatic hydrocarbons (PAHs) in the atmosphere over the Central Himalayas. *Aerosol and Air Quality Research, 17*(12), 2942–2954. https://doi.org/10.4209/aaqr.2016.09.0385

Cigánková, H., Mikuška, P., Hegrová, J., Pokorná, P., Schwarz, J., & Krajčovič, J. (2021a). Seasonal variation and sources of elements in urban submicron and fine aerosol in Brno, Czech Republic. *Aerosol and Air Quality Research, 21*(5), 200556. https://doi.org/10.4209/aaqr.2020.09.0556

Cigánková, H., Mikuška, P., Hegrová, J., Krajčovič, J. (2021b). Comparison of oxidative potential of PM1 and PM2.5 urban aerosol and bioaccessibility of associated elements in three simulated lung fluids. Science of The Total Environment, 800, 149502. https://doi.org/10.1016/j.scitotenv.2021b.149502.

Decesari, S., Facchini, M. C., Carbone, C., Giulianelli, L., Rinaldi, M., Finessi, E., Fuzzi, S., Marinoni, A., Cristofanelli, P., Duchi, R., Bonasoni, P., Vuillermoz, E., Cozic, J., Jafferzo, J. L., & Laj, P. (2010). Chemical composition of PM10 and PM1 at the highaltitude Himalayan station Nepal Climate Observatory-Pyramid (NCO-P) (5079 m a.s.l.). *Atmospheric Chemistry and Physics, 10*, 4583–4596. https://doi.org/10.5194/acp-10-4583-2010

Dokiya, Y., Maruta, E., Yoshikawa, T., Ishimori, H., & Tsurumi, M. (1992). Chemical species in the deposition at some peaks of the Himalaya. *Environmental Science, 5*, 109–114.

Filonchyk, M., & Yan, H. (2018). The characteristics of air pollutants during different seasons in the urban area of Lanzhou. *Northwest China. Environmental Earth Sciences, 77*, 763. https://doi.org/10.1007/s12665-018-7925-1

Global Air, 2020. State of Global Air 2020 reports air pollution's impact on neonatal mortality. https://www.healthheffects.org/announcements/state-global-air-2020-reports-air-pollutions-impact-neonatal-mortality.

Giri, D., Murthy, V.K., Adhikary, P.R., Chhetri, R.B., Khanal, S.N., Sharma, C.K. (2004). Descriptive statistical analysis of PM10 values in selected air monitoring sites in Kathmandu Valley. RONAST, Nepal.

Giri, D., Murthy, V. K., Adhikary, P. R., & Khanal, S. N. (2007). Estimation of number of deaths associated with exposure to excess ambient PM10 air pollution. *International Journal of Environmental Science and Technology, 4*, 183–188. https://doi.org/10.1007/BF03326272

Giri, D., Murthy, V. K., & Adhikary, P. R. (2008). The influence of meteorological conditions on PM10 concentrations in Kathmandu Valley. *International Journal of Environmental Research, 2*(1), 49–60. https://doi.org/10.22059/ijer.2010.175

Gong, P., Wang, X., & Yao, T. (2011). Ambient distribution of particulate-and gas-phase n-alkanes and polycyclic aromatic hydrocarbons in the Tibetan Plateau. *Environmental Earth Sciences, 64*, 1703–1711. https://doi.org/10.1007/s12665-011-0974-3

Gurung, A., Michelle L. Bell, L. M. (2013). The state of scientific evidence on air pollution and human health in Nepal. Environmental Research, 124, 54–64. https://doi.org/10.1016/j.envres.2013.03.007.

International Commission on Radiological Protection (1994). Human respiratory tract model for radiological protection; International Commission on Radiological Protection: Stockholm, Sweden, 1994.

International Journal of Environmental Analytical Chemistry, 89(2), 67–82. https://doi.org/10.1080/03067310802526985

Jha, P. K., & Lekhak, D. K. (2003). Air pollution studies and management efforts in Nepal. *Pure and Applied Geophysics, 160*, 341–348. https://doi.org/10.1007/s00024-003-8782-7

Karbowska, B. (2016). Presence of thallium in the environment: sources of contaminations, distribution and monitoring methods. Environmental Monitoring and Assessment, 188(640). https://doi.org/10.1007/s10661-016-5647-y.

Kim, K. H., Kabir, E., & Kabir, S. (2015). A review on the human health impact of airborne particulate matter. *Environment International, 74*, 136–143. https://doi.org/10.1016/j.envint.2014.10.005

Kishida, M., Mio, C., Imamura, K., Kondo, A., Kaga, A., Shrestha, M.L., Takenaka, N., Maeda, Y., Sapkota, B., Fujimori, K., Shibutani, Y., Bandow, H. (2009). Temporal variation of atmospheric polycyclic aromatic hydrocarbon concentrations in PM10 from the Kathmandu Valley and their gas-particle concentrations in winter.

Křůmal, K., & Mikuška, P. (2020). Mass concentrations and lung cancer risk assessment of PAHs bound to PM1 aerosol in six industrial, urban and rural areas in the Czech Republic, Central Europe. *Atmospheric Pollution Research, 11*, 401–408. https://doi.org/10.1016/j.apr.2019.11.012

Křůmal, K., Mikuška, P., & Večeřa, Z. (2013). Polycyclic aromatic hydrocarbons and hopanes in PM1 aerosols in urban areas. *Atmospheric Environment, 67*, 27–37. https://doi.org/10.1016/j.atmosenv.2012.10.033

Křůmal, K., Mikuška, P., & Večeřa, Z. (2017). Characterization of organic compounds in winter PM1 aerosols in a small industrial town. *Atmospheric Pollution Research, 8*, 930–939. https://doi.org/10.1016/j.apr.2017.03.003

Kumar, P., Morawska, L., Martani, C., Biskos, G., Neophytou, M., Di Sabatino, S., Bell, M., Norford, L., & Britter, R. (2015). The rise of low-cost sensing for managing air pollution in cities. *Environment International, 75*, 199–205. https://doi.org/10.1016/j.envint.2014.11.019

Lakhani, A. (2012) Source apportionment of particle bound polycyclic aromatic hydrocarbons at an industrial location in Agra, India. *The Scientific World Journal*, p. 10. https://doi.org/10.1100/2012/781291

Lewis, A.C., Von Schneidemesser, E., Peltier, R.E. (2018). Low-cost sensors for the measurement of atmospheric composition: overview of topic and future applications. WMO-No.121. World Meteorological Organisation. orcid.org/0000–0002–4075–3651.

Majumder, A. K., Nazmul Islam, K. M., Bajracharya, R. M., & Carter, W. S. (2012). Assessment of occupational and ambient air quality of traffic police personnel of the Kathmandu valley, Nepal; in view of atmospheric particulate matter concentrations (PM10). *Atmospheric Pollution Research, 3*(1), 132–142. https://doi.org/10.5094/APR.2012.013

Masiol, M., Hofer, A., Squizzato, S., Piazza, R., Rampazzo, G., & Pavoni, B. (2012). Carcinogenic and mutagenic risk associated to airborne particle-phase polycyclic aromatic hydrocarbons: A source apportionment. *Atmospheric Environment, 60*, 375–382. https://doi.org/10.1016/j.atmosenv.2012.06.073

McKercher, G. R., Salmond, J. A., & Vanos, J. K. (2017). Characteristics and applications of small, portable gaseous air pollution monitors. *Environmental Pollution, 223*, 102–110. https://doi.org/10.1016/j.envpol.2016.12.045

Meteoblue (2006–2022). Počasí Brno. Meteoblue. Retrieved November 2019 from www.meteoblue.com/cs/po%C4%8Das%C3%AD/t%C3%BDden/tuls%c4%abpur_nep%c3%a1l_1282635.

Mikuška, P., Křůmal, K., & Večeřa, Z. (2015). Characterization of organic compounds in the PM2.5 aerosols in winter in an industrial urban area. *Atmospheric Environment, 105*, 97–108. https://doi.org/10.1016/j.atmosenv.2015.01.028

Mikuška, P., Vojtěšek, M., Křůmal, K., Mikušková-Čampulová, M., Michálek, J., & Večeřa, Z. (2020). Characterization and source identification of elements and water-soluble ions in submicrometre aerosols in Brno and Šlapanice (Czech Republic). *Atmosphere, 11*(7), 688. https://doi.org/10.3390/atmos11070688

Nasir, Z. A., Colbeck, I., Ali, Z., & Ahmed, S. (2015). Heavy elements composition of particulate matter in rural residential built environments in Pakistan. *The Journal of Animal & Plant Sciences, 25*(3), 706–712.

Nazir, R., Shaheen, N., & Shah, M. H. (2011). Indoor/outdoor relationship of trace elementss in the atmospheric particulate matter of an industrial area. *Atmospheric Research, 101*(3), 765–772. https://doi.org/10.1016/j.atmosres.2011.05.003

Pokhrel, B., Gong, P., Wang, X., Wang, Ch., & Gao, S. (2018). Polycyclic aromatic hydrocarbons in the urban atmosphere of Nepal: Distribution, sources, seasonal trends, and cancer risk. *Science of the Total Environment, 618*, 1583–1590. https://doi.org/10.1016/j.scitotenv.2017.09.329

Rajput, P., Sarin, M., & Kundu, S. (2013). Atmospheric particulate matter (PM2.5), EC, OC, WSOC and PAHs from NE-Himalaya: abundances and chemical characteristics. *Atmospheric Pollution Research, 4*(2), 214–221.

Rajput, P., Sarin, M., Sharma, D., & Singht, D. (2014). Atmospheric polycyclic aromatic hydrocarbons and isomerratios as tracers of biomass burning emissions in Northern India. *Environmental Science and Pollution Research, 21*, 5724–5729. https://doi.org/10.1007/s11356-014-2496-5

Ramanathan, V., Ramana, M.V. (2007). Characterization of the seasonal cycle of South Asian aerosols: a regional-scale modeling analysis. Journal of Geophysical Research. Atmosphere, 112, /https://doi.org/10.1029/2006JD008143.

Ravindra, K., Ranjeet, S., & Van Grieken, R. (2008). Atmospheric polycyclic aromatic hydrocarbons: Source attribution, emission factors and regulation. *Atmospheric Environment, 42*(13), 2895–2921. https://doi.org/10.1016/J.ATMOSENV.2007.12.010

Sahu, R., Dixit, K. K., Mishra, S., Kumar, P., Shukla, A. K., Sutaria, R., Tiwari, S., & Tripathi, S. N. (2020). Validation of low-cost sensors in measuring real-time PM10 concentrations at two sites in Delhi National Capital Region. *Sensors, 20*(5), 1347. https://doi.org/10.3390/s20051347

Saud, B., Paudel, G. (2018). The threat of ambient air pollution in Kathmandu, Nepal. Journal of Environmental and Public Health, 2018, Article ID 1504591, https://doi.org/10.1155/2018/1504591.

Schroeder, W. H., Dobson, M., Kane, D. M., & Johnson, N. D. (1987). Toxic trace elements associated with airborne particulate matter: A review. *Journal of Air and Waste Management Association, 37*, 1267–1285. https://doi.org/10.1080/08940630.1987.10466321

Seinfeld, J.H.; Pandis, S.N. Atmospheric chemistry and physics. From Air Pollution to Climate Change; Wiley & Sons: New York, NY, USA, 1998.

Sellegri, K., Laj, P., Venzac, H., Boulon, J., Picard, D., Villani, P., Bonasoni, P., Marinoni, A., Cristofanelli, P., & Vuillermoz, E. (2010). Seasonal variations of aerosol size distributions based on long-term measurements at the high altitude Himalayan site of Nepal Climate Observatory-Pyramid (5079 m). *Nepal. Atmospheric Chemistry and Physics, 10*(21), 6537–6566. https://doi.org/10.5194/acp-10-10679-2010

Sill, M., Kirkby, J. (2013). Atlas of Nepal in the Modern World (Sustainable Development Set Book 4). 164 p.

Simoneit, B., Medeiros, P. M., & Didyk, B. (2005). Combustion products of plastics as indicators for refuse burning in the atmosphere. *Environmental Science & Technology, 39*(18), 6961–6970. https://doi.org/10.1021/es050767x

Tasić, V., Kovačević, R., Maluckov, B., Apostolovski-Trujić, T., Matić, B., Cocić, M., & Šteharnik, M. (2017). The content of As and heavy metals in TSP and PM10 near Copper smelter in Bor, Serbia. *Water, Air and Soil Pollution, 228*, 230. https://doi.org/10.1007/s11270-017-3393-6

Torres, O., Jethva, H., Ahn, C., Jaross, G., & Loyola, D. G. (2020). TROPOMI aerosol products: Evaluation and observations of synoptic-scale carbonaceous aerosol plumes during 2018–2020. *Atmospheric Measurement Techniques, 13*(12), 6789–6806. https://doi.org/10.5194/amt-13-6789-2020

Tyagi, V., Gurjar, B. R., Joshi, N., & Kuma, P. (2012). PM10 and heavy elementss in suburban and rural atmospheric environments of Northern India. *Journal of Hazardous, Toxic, and Radioactive Waste, 16*(2), 175–182. https://doi.org/10.1061/%28ASCE%29HZ.2153-5515.0000101

Viana, M., Kuhlbusch, T. A. J., Querol, X., Alastuey, A., Harrison, R. M., Hopke, P. K., Winiwarter, W., Vallius, M., Szidat, S., Prévôt, A. S. H., Hueglin, C., Bloemen, H., Wåhlin, P., Vecchi, R., Miranda, A. I., Kasper-Giebl, A., Maenhaut, W., & Hitzenberger, R. (2008). Source apportionment of particulate matter in Europe: A review of methods and results. *Journal of Aerosol Science, 39*(10), 827–849. https://doi.org/10.1016/j.jaerosci.2008.05.007

Waldorf, D. (2018, March 16). NEPAL Systematic Country Diagnostic. A new approach for a federal Nepal. The World Bank, Washington. Retrieved November 2018, from https://www.worldbank.org/en/region/sar/publication/systematic-country-diagnostic-a-new-approach-for-a-federal-nepal.

Wang, G., Kawamura, K., Xie, M., Hu, S., Gao, S., Cao, J., An, Z., & Wang, Z. (2009). Site-distribution of n-alkanes, PAHs and hopanes in the urban, mountain and marine atmosphere over East Asia. *Atmospheric Chemistry and Physics, 9*(22), 8869–8882. https://doi.org/10.5194/acp-9-8869-2009

Wang, T., Xia, Z., Wu, M., Zhang, Q., Sun, S., Yin, J., Zhou, Y., & Yang, H. (2017). Pollution characteristics, sources and lung cancer risk of atmospheric polycyclic aromatic hydrocarbons in a new urban districts of Nanjing, China. *Journal of Environmental Sciences, 55*, 118–128. https://doi.org/10.1016/j.jes.2016.06.025

World Health Organization (2002). Air quality guidelines for Europe, 2nd edition. World Health Organization, 91. Regional office for Europe. Retrieved August, 2019f from https://apps.who.int/iris/handle/10665/107335.

World Health Organization (2006). Air quality guidelines, Global update 2005. World Health Organisation. Retrieved July 2021 from https://www.euro.who.int/__data/assets/pdf_file/0005/78638/E90038.pdf

World Health Organization (2014). World health statistics 2014. World Health Organization. Retrieved Juny 2020 from https://digitallibrary.un.org/record/3868753.

Yu, Y., Panday, A., Hodson, E., Galle, B., & Prinn, R. (2008). Monocyclic aromatic hydrocarbons in Kathmandu during the winter season. *Water, Air and Soil Pollution, 191*, 71–81. https://doi.org/10.1007/s11270-007-9607-6

Yunker, M., Macdonald, R., Vingarzan, R., Mitchell, R., Goyette, D., & Sylvestre, S. (2002). PAHs in the Fraser River basin: A critical appraisal of PAH ratios as indicators of PAH source and composition. *Organic Geochemistry, 33*(4), 489–515. https://doi.org/10.1016/S0146-6380(02)00002-5